A STUDY OF MICROMEGAS WITH PREAMPLIFICATION WITH A SINGLE GEM

S. KANE, J. MAY, J. MIYAMOTO, I. SHIPSEY
Dept of Physics, Purdue University, W. lafayette, IN 47906, USA

S. ANDRIAMONJE, A. DELBART, J. DERRE, I. GIOMATARIS,
F. JEANNEAU
CEA/DSM/DAPNIA, CE-Saclay, 91191 Gif-sur-Yvette, France

A MICROMEGAS detector was combined with a single GEM to allow preamplification before primary electrons enter the main detector. The preamplification not only extends the maximum achievable gas gain without discharge but also it minimizes spark rates when exposed to high intensity ionizing particles. We performed both laboratory and beam tests with various gas mixtures to find optimal operational characteristics and the results were encouraging and this particular combination may be suitable for experiments that require high counting rates and good spatial resolution as in VLHC.

1 Introduction

A MICROMEGAS is a robust miropatterned gaseous detector with minimal insulator between the anode and the cathode [1]. The detector will be used by the COMPASS experiment at CERN [2]. The detector is not constructed on one plane as in other substrate-based micropatterned devices(e.g. MSGC) but the a thin metallic mesh is placed above the anode readout plane. There is a small amplification gap between the anode and the cathode. The small amplification gap is created by small Kapton pillars (50 μm thick). The pillars prevent the mesh from sagging or touching the anode and from causing short circuit. The electric field lines in the amplification gap are similar (except near the holes) to a parallel plate gas chamber. Because the MICROMEGAS gap is small, it does not require large bias to achieve reasonable gas gain whereas in a parallel plate gas chamber the bias voltage required is prohibitively high as the amplification gas used is typically a few millimeters.

An early version of MICORMEGAS was a simple metal mesh supported by polyimide pillars glued on the anode plane but today there is a new type of micromesh [3]. The MICROMEGAS in this study employes a new micromesh which was fabricated entirely by the Kapton photolithography technique used in the GEM production [4] The final micromesh resembles a one-sided GEM with many etched holes to allow the primary ionization to enter the amplification gap [5]. The metallized surface on the mesh and the anode plane creates a strong electric field to cause electron multiplication in the gap. The pillars that support the micromesh are residual Kapton that were not etched away in the lithography processes. The decoupling of the amplification gap and the drift field makes the proportional mode possible. As in the GEM, there are plenty of holes to have good electron transparency and 20% of electron transparency has been reported [3]. The pillars on the mesh have a pitch of 1-2 mm and each pillar's diameter is about 80 μm. These pillars inevitably create dead areas but the blocked areas are insignificant.

Even though the MICROMEGAS has been known to be very radiation hard and robust in high intense radiation, adding a preamplification device can improve its performance significantly [6]. Preamplification by a single GEM seems ideal to accomplish the goal because the MICROMEGAS itself has high gas gain. The addition of the single GEM preamplification relaxes the operation conditions of the whole system and leads to a spark-free condition as described later.

2 Detector

Our detector consists of mainly the anode plane, micromesh with pillars, a single GEM and the drift mesh. The details of the detector structure and the distance between the micromesh, GEM and drift plane are shown in Figure 1. The drift mesh is located above the GEM foil and any electrons created between the GEM and the drift mesh experience two amplification stages: 1. GEM and 2. MICROMEGAS. It is possible for some electrons to be created below the GEM in which case they experience only one stage of amplification, namely MICROMEGAS alone. In order to study this effect it is possible to isolate events with no preamplification by switching off the drift voltage and use the lower electrode of the GEM as a drift mesh (pure MICROMEGAS mode). The GEM was biased by a resistor chain but the micromesh was biased through a charge sensitive preamplifier which reads out the signals (see fig 2). With the conventional preamplifier with a rise time of a few hundred nano seconds, a large part of the signal is formed by slowly moving ions traveling in the amplification gap. However the distance the ions have to cover to induce signals is only 50 to 100 μm and the slowly moving ions are quickly evacuated minimizing the space charge effect. Another advantage is that most ions are collected by the micromesh preventing the majority of ions from entering the drift space. Therefore, the MICROMEGAS detector has a high rate capability and 10E+7 Hz at gain of 10E+3 has been reported [6]. This is an attractive feature which is useful in a TPC (time projection chamber) where ions returning to the drift region should be minimized so as not to

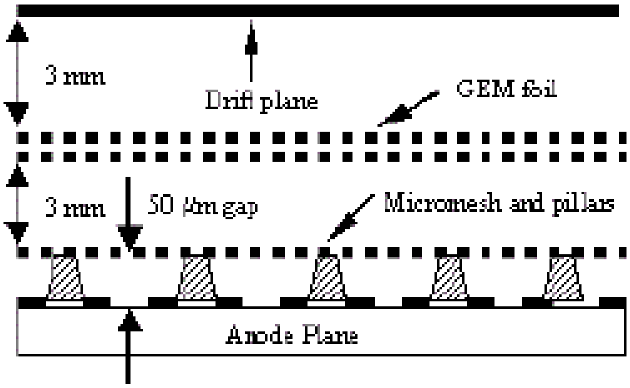

Figure 1. A schematic of MICROMEGAS+GEM with their dimensions

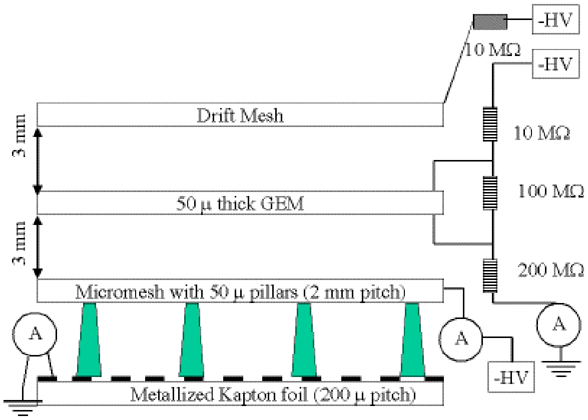

Figure 2. MICROMEGAS+GEM bias scheme

distort the electric field in the drift volume [7].

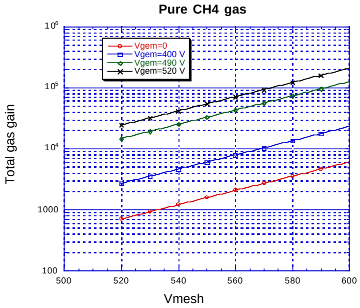

Figure 3. Absolute gas gain in pure CH_4

3 Gas gain in various gas mixtures

Gas gain was measured with a Fe-55 source in pure CH_4, Ar-DME(9:1), Ar-CO_2(7:3) and Ne-CF_4-Isobutaine(79:10:11) and plotted as a function of voltage on the MICROMEGAS with various parametrized GEM voltages in figures 3-6. In each case (except Ar-CO_2), the gain was also measured with no GEM preamplification (Vgem=0). In most gases GEM preamplification can easily push the gas gain to the $10E+4$ region while it is not easy to reach this region with MICROMEGAS alone. In a low gas gain mixture like Ar-CO_2, it is not possible to achieve useful gas gain for minimum ionization detection without GEM preamplifcation. In the light gas mixture, Ne-CF_4-Isobutane, $10E+5$ was achieved. This is an indication that this mixture would give very few sparkes in intense radiation and its property will be discussed later.

4 Energy spectra with a Fe-55 X-ray source

Energy resolution was measured with and without GEM preamplification by taking pulse height spectra of a 3 mm uncollimated Fe-55 X-ray source in an Ar-DME(9:1) mixture. Because the energy resolution is a function of gas gain, measurements were taken at similar gas gain. On the left side of figure 7, the

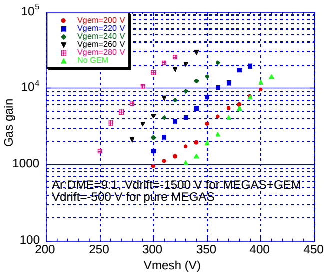

Figure 4. Absolute gas gain in pure Ar-DME(9:1)

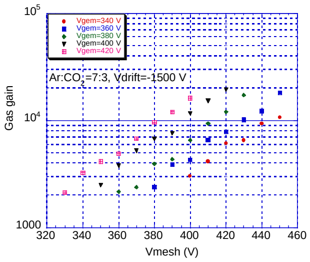

Figure 5. Absolute gas gain Ar-CO$_2$(9:1)

pulse height spectrum for the pure MICROMEGAS is plotted. Its energy resolution was calculated from Gaussian fitting and it was about 32 %(FWHM). Contributions to the energy resolution include possible geometrical variations of the area illuminated by the source.

Another pulse height spectrum was taken with GEM preamplification in a similar condition and plotted on the right side of figure 7. The energy resolution was about 30 % (FWHM) demonstrating that there was no significant degradation in energy resolution caused by the GEM preamplification. The small peak seen between the noise peak and the argon escape peak is probably attributable to primary ionization created between the GEM and the MICROMEGAS. These primary electrons experience amplification only once

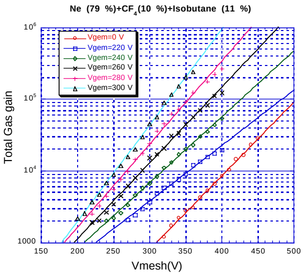

Figure 6. Absolute gas gain in Ne-CF$_4$-Isobutane (79:10:11)

which produces a much lower pulse height which appears as a lower energy photon in figure 7.

Also interesting is the effect of the transfer E-field on the energy resolution. The transfer E-field is defined as an electric field between the micromesh and the GEM lower electrode. If this field is too low (the GEM lower electrode and the micromesh have similar voltage), the electrons amplified in the GEM do not quickly reach the MICROMEGAS for secondary amplification. These electrons are lost to the GEM lower electrode. On the other hand, if the field is too strong, many electrons are collected by the micromesh and they are again lost. The number of electrons lost to either device (GEM lower electrode or micromesh) influences mainly gas gain but also the shape of the Gaussian spectra as well. Pulse height spetra were measured by various transfer E-field values and plotted in figure 8. The gas gain (proportional to the peak position) increased with the transfer E-field but it reached saturation and no longer grew indicating that the electron transfer efficiency reached the maximam point. Another interesting feature is that the Gaussian shape is assymetrical (long tail) with a lower tranfer E-field as one can see in the first two pulse height spectra. There are more events in the higher energy region and the tail on that side is visible. This tail on the high energy side disappears once the transfer E-field is sufficiently high and the Gaussian shape is more or less symmetric. This is probably because with a lower E-field, avalanche electrons exiting near the center of the GEM holes and those exiting slightly off the center have distinct kinetic energies of electrons before they reach the MICROMEAGS. This geometrical inhomogeniuity is minimal once the transfer E-field is high because there are now many electric field lines in the GEM

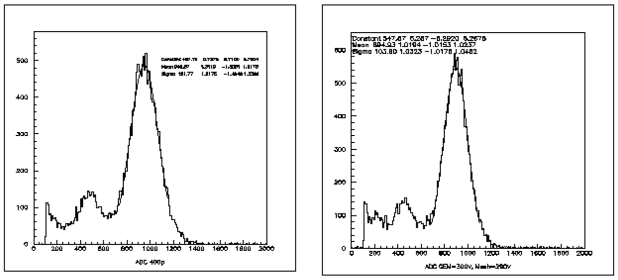

Figure 7. Left plot:Pulse height spectrum for MICROMEGAS only, Vmesh=400V, Vdrift=-500, dE/E=32 (FWHM) %. Right plot: Pulse height spectrum for MICROMEGAS+GEM, Vmesh=290V, Vgem=300V, Vdrift=-1500V, dE/E=30(FWHM)%.

pointing to the MICROMEGAS rather than to the GEM lower electrodes.

5 Beam test

The limitation of most micropatterned gas detectors comes from the fact that sparks are easily formed inside the small amplification gap once heavily ionizing particles pass through them. The energy released from this event is large enough to damage the thin electrodes causing failure of the affected area. Many studies show that dividing the total gas gain into several stages using more than one amplification device(e.g. GEM+MSGC etc) minimizes spark rates.

Because the MICROMEGAS has minimal insulation materials in the amplification gap, it may be more robust than other fragile micropatterned detectors. It has been previously reported that adding preamplificaiton above the micromesh is an effective way to minimize spark rates in a MICROMEGAS in an intense radiation enviroment where heaviy ionizing particles are present [6]. In that study the preamplification was realized by applying extremely high voltage on the drift mesh to create an intense electric field in the drift region. Once the electric field reaches a certain value, electrons begin the multiplifcaiton process in the drift space. The extra amplification eases the gain requirements on the MICROMEGAS and prevents it from satisfing the Raether condition. However the drift region is not optimal for preamplification as it is large (a few millimeters) and the voltage required to cause an avalanche is consequently high. Preamplification by a GEM is more efficient and the combined detector does not need elaborate insulation as in the case of pream-

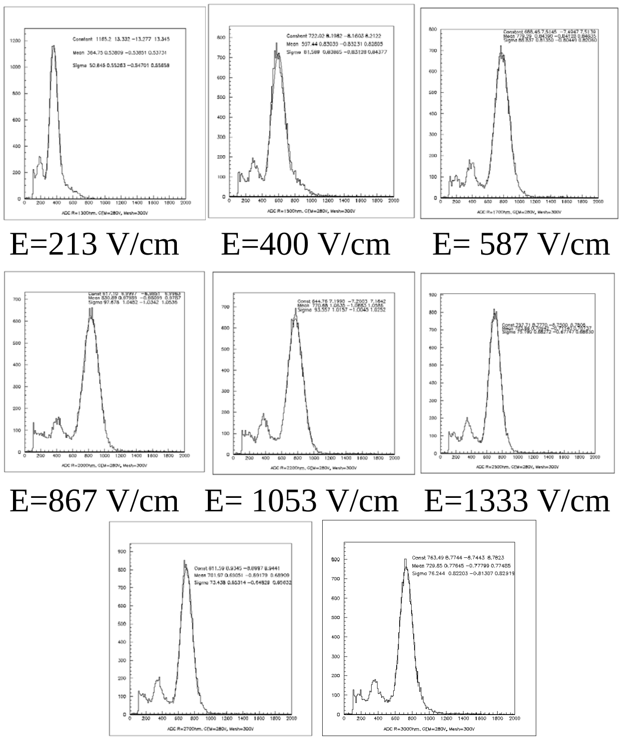

E=213 V/cm E=400 V/cm E= 587 V/cm

E=867 V/cm E= 1053 V/cm E=1333 V/cm

E=1520 V/cm E=1800 V/cm

Figure 8. Pulse height spectra with varied tranfer E-field. Vmesh=300V, Vgem=280V.

plification in the drift space.

We performed a beam test at CERN's LHC-b facility in a high flux 10 GeV/c proton beam to measure the spark rates of the MICROMEGAS+GEM in different gas mixtures. This beam size is about 2 cm x 2 cm and triggering was done by a large scintillator so as not to miss any incoming protons on the MICROMEGAS. The maximum beam intensity was $10E+6$ protons/spill and the spill lasted about 300 $msec$. The tracking ability of the MICROMEAGS was previously reported in ref [2] in detail and our study mainly concentrated on spark rates in different gas mixtures.

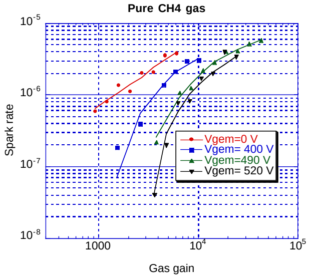

Figure 9. Spark rates in CH_4 gas as a function of gas gain.

The methodology to measure the spark rates is the following. When discharge occurs in the detector, unusually high current is drawn from the power supply connected to the micromesh(the anode is grounded). This unusually high current lasts a few hundred milliseconds because photon feedback plays some roles and the current does not terminate immediately. Thus a 100 $msec$ gate was imposed on the scaler's time window not to double count spark rates. The number of protons arriving on the detector was counted from the triggered events with the scintillator and the number of sparks was counted on a scaler. The ratio of the two values gives the spark rate. Our measurements were done in two different gas mixtures (pure CH_4 and Ne-CF_4-Isobutane (79:10:11)). In figure 9, spark rates in CF_4 are plotted as a function of gas gain. Spark rates were lowered by using the GEM and with GEM voltage=520 V it was possible to achieve $10E-8$ spark rate (almost spark free region). This voltage value on the GEM is however dangerously high and now the GEM may be prone to damage. A good solution to this problem is to use ligher gas mixture based on Neon. In figure 10, spark rates for the Ne-CF_4-Isobutane mixture were plotted. The improvement is obvious and even with a low GEM voltage=300V, it was possible to achieve spark rates as low as $10E-8$ and still gas gain was $10E+5$ which is more than enough to detect minimum ionization particles.

6 Conclusion

The GEM preamplification added to the MICROMEGAS proved to be beneficial to reduce spark rates and spark rates as low as $10E-8$ were achieved in

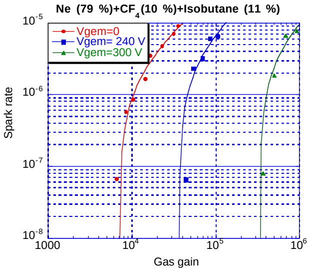

Figure 10. Spark rates in Ne-CF_4-Isobutane (79:10:11) as a function of gas gain.

Ne-CF_4-Isobutane mixture with a low GEM voltage. The GEM preamplification did not significantly degrade the energy resolution of the MICROMEGAS and the combination of the two is a suitable technology for a large tracker at a future high energy accelerator such as an upgrade to the LHC or a new machine such as the VLHC. The device is also ideal for readout of a TPC at a high energy Linear Collider and finally due to the low spark rate it is idea for low background applications such as WIMP/axion searches and for neutrino physics.

Acknowledgments

The GEM foils used in this work were provided by F. Sauli at CERN.

References

1. I. Giomataris *et al.*, Nucl. Instr. and Meth. **A376**, 29-35 (1996).
2. D. Thers *et al.*, Nucl. Instr. and Meth. **A469**, 133-146 (2001).
3. A. Delbart *et al.*, Nucl. Instr. and Meth. **A461**, 84-87 (2001).
4. F. Sauli, Nucl. Instr. and Meth. **A386**, 531-534 (1997).
5. H.S. Cho *et al.*, IEEE. Trans. Nucl. Sci. **46(3)**, 306-311 (1999).
6. G. Charpak *et al.*, presented at Vienna conference on instrumentation, Vienna, 2001.
7. TELSA technical design report, DESY 2001-11, TESLA Report 2001-23, TESLA-FEL-2001-05.